Interfacial waviness during condensation heat transfer

Interfacial waviness during condensation heat transfer

A Berto[1], P Lavieille[2], M Azzolin[1], S Bortolin[1], M Miscevic[2] and D Del Col[1]

[1] Department of Industrial Engineering, University of Padova
Via Venezia 1, 35131 – Padova, Italy
[2] Université Paul Sabatier – Laboratoire Plasma et Conversion d'Energie
UMR CNRS-INP-UPS 5213, 118 Route de Narbonne, Toulouse, France

Corresponding author: Arianna Berto; e-mail: arianna.berto@unipd.it

Abstract. Heat transfer coefficients and liquid film thickness have been measured during convective condensation inside a 3.4 mm internal diameter channel. Condensation tests have been run with refrigerant R245fa during vertical downflow at mass velocity equal to 50 kg m^{-2} s^{-1} and 100 kg m^{-2} s^{-1}. The test section is composed of two heat exchangers for the measurement of the heat transfer coefficient connected by means of a glass tube designed for the visualization of the two-phase flow patterns and for the measurement of the liquid film thickness. The liquid film thickness is determined by coupling a shadowgraph technique and chromatic confocal measurements. The measured values of heat transfer coefficient and liquid film thickness are reported and analysed together to investigate the effect of waves on the condensation heat transfer mechanisms.

1. Introduction

Annular flow is one of the most recurrent flow regimes encountered during condensation in vertical channels. In annular flows, the heat transfer mainly depends on the vapour shear stress, the condensate film thickness and the turbulence in the liquid film (Toninelli et al. [1], Azzolin et al. [2]). An accurate measurement of the liquid film thickness is important not only for the characterization of the two-phase flow in terms of void fraction and phases velocities but also for better understanding the condensation heat transfer mechanisms. Most of the studies dealing with liquid film thickness measurements concern relatively big channels (20-30 mm diameter) and air-water mixtures (Cioncolini et al. [3]). There is a lack of data taken with refrigerants in saturated conditions and inside small channels due to the technical difficulties in performing accurate measurements at such scales. A comprehensive review of methods employed in micro-scale for the measurement of the liquid film thickness and related literature is provided by Tibiriçá et al. [4]. Among the optical techniques, Mederic et al. [5] measured local liquid film thickness and local void fraction by means of image analysis during condensation of n-pentane inside a 0.56 mm inner diameter borosilicate tube. Han et al. [6] performed liquid film thickness measurements during annular flow by means of laser confocal displacement meter using degassed water and air in glass tubes with inner diameters of 0.3, 0.5 and 1.0 mm. None of these works involves refrigerants. In the present paper, condensation heat transfer of R245fa inside a 3.4 mm inner diameter tube is studied during vertical downflow at 40 °C saturation temperature and mass fluxes equal to 50 and 100 kg m^{-2} s^{-1}. Heat transfer coefficient and liquid film thickness measurements have been performed, together with flow pattern visualizations.

2. Experimental test rig and data reduction

The test rig consists of a primary refrigerant loop and three auxiliary water loops ([2]). In the refrigerant loop, a post-condenser is used to keep the refrigerant subcooled before it enters a magnetic driven gear pump. A tube-in-tube heat exchanger is used to vaporize and superheat the fluid. After the evaporator, the refrigerant enters the condensation test section which is composed of two counter-current heat exchangers for heat transfer measurements separated by a 40 mm long borosilicate glass tube for flow pattern visualization and liquid film thickness measurement. Each heat exchanger is divided respectively in three and two sectors: the refrigerant flows in the internal circular channel (3.4 mm diameter), while the water streams in the external annulus. A finned geometry has been machined on the coolant side to decrease the water heat transfer resistance and accommodate wall thermocouples. In each sector six thermocouples are embedded in the copper wall for a total of 30 wall thermocouples installed in the test section. On the water side, two thermocouples and a triple-junction thermopile are used to check the temperature difference of the water between inlet and outlet of each sub-sector. Three Coriolis mass flow meters are employed to measure the water and refrigerant mass flow rates. The refrigerant temperatures at the inlet and outlet of the test section are measured by T-type thermocouples, while the inlet pressure is measured using relative pressure transducers. The pressure drop along the test section is determined by two differential pressure transducers with different full scale. The experimental internal heat transfer coefficient in the *i*-th sector is obtained as follows:

$$\mathrm{HTC}_i = \frac{q_{water,i}}{A\cdot\left(T_{sat}-T_{w,m}\right)_i} = \frac{\dot{m}_{water,i}\cdot c_{water}\cdot\Delta T_{water,i}}{A\cdot\left(T_{sat}-T_{w,m}\right)_i} \tag{1}$$

where A is the internal heat transfer area, T_{sat} and $T_{w,m}$ are respectively the saturation and mean wall temperature, the latter intended as the average of the two temperatures measured in the middle of the sector, $q_{water,i}$ is the heat flow rate exchanged in each *i*-th sector (evaluated by means of a heat balance on the water side), $\dot{m}_{water,i}$ is the measured water mass flow rate and $\Delta T_{water,i}$ is the water temperature difference between inlet and outlet measured by the *i*-th thermopile. The heat flow rate is employed to determine the enthalpy at the outlet of the *i*-th sector (from the measured refrigerant mass flow rate and the inlet enthalpy) and thus the outlet vapour quality. The thermodynamic properties of R245fa are computed using REFPROP 9.1 (Lemmon et al. [7]). Considering the present experimental database, the mean expanded uncertainty of the heat transfer coefficient (with a coverage factor equal to 2) is 3.1%.

The external side of the glass tube has been designed to detect and magnify the liquid film thickness on a camera working in a shadowgraph configuration. The liquid film thickness is deduced from calibration curves obtained by coupling the shadowgraph technique, through which the vapour-liquid interface can be detected from the recorded images using a ray tracing model, and a confocal chromatic sensor, which allows to measure liquid film thicknesses up to 300 μm provided that the slope of the interface is lower than 28°. The standard uncertainty of the film thickness is about ±2 μm in the case of the confocal sensor measurements, while it ranges between ±10 μm and ±15 μm if using the shadowgraph technique. Additional information about the present technique is reported in Berto et al. [8].

3. Experimental results

Flow pattern visualizations have been recorded using Photron® FASTCAM Mini UX100 High Speed Camera, coupled with Navitar® Zoom 7000 18-108 mm Macro Lens and a LED illumination system. Images have been recorded at 1000 fps. Annular flow has been observed for all the operative conditions with R245fa (Figure 1). The interface, depending on vapour quality and mass velocity, is rippled by waves of different amplitude and frequency. At vapour quality x = 0.52, the vapour-liquid interface in the case of G = 100 kg m^{-2} s^{-1} is much more stirred by interfacial waves compared to G = 50 kg m^{-2} s^{-1}. Probability density function (PDF) is used to characterize the amplitude of observed interfacial waves. Figure 2 reports the probability density function of the measured liquid film thickness at 50 and 100 kg m^{-2} s^{-1} and at two vapour quality values (x = 0.3 and x = 0.7). The range of detected liquid film thicknesses reduces as the vapour quality increases. In particular, at G = 100 kg m^{-2} s^{-1} the maximum detected liquid film thickness is around 1000 μm at x = 0.3 while it is equal to 345 μm at x = 0.7.

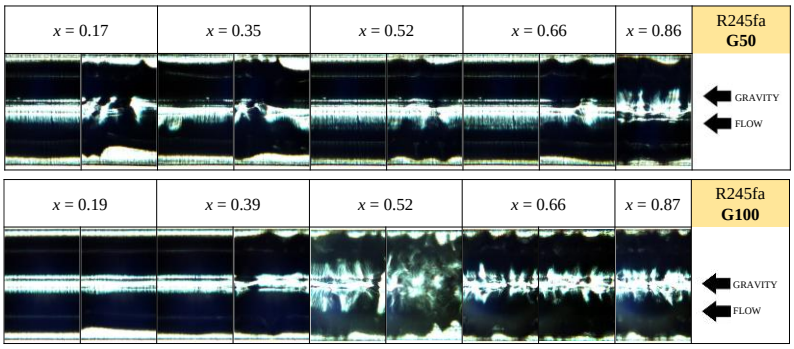

Figure 1. Flow pattern visualizations during vertical downward condensation of R245fa at 40 °C saturation temperature, mass velocity G equal to 50 and 100 kg m^{-2} s^{-1} and various vapor qualities.

However, looking at the PDFs, the occurrence of such high film thickness values is rare and the most probable film thickness is found to be well below 200 μm for all the investigated conditions. Furthermore, the most probable film thickness shifts towards lower values when increasing the mass velocity and this is related to the reduction of mean film thickness due to increased vapour shear stress.

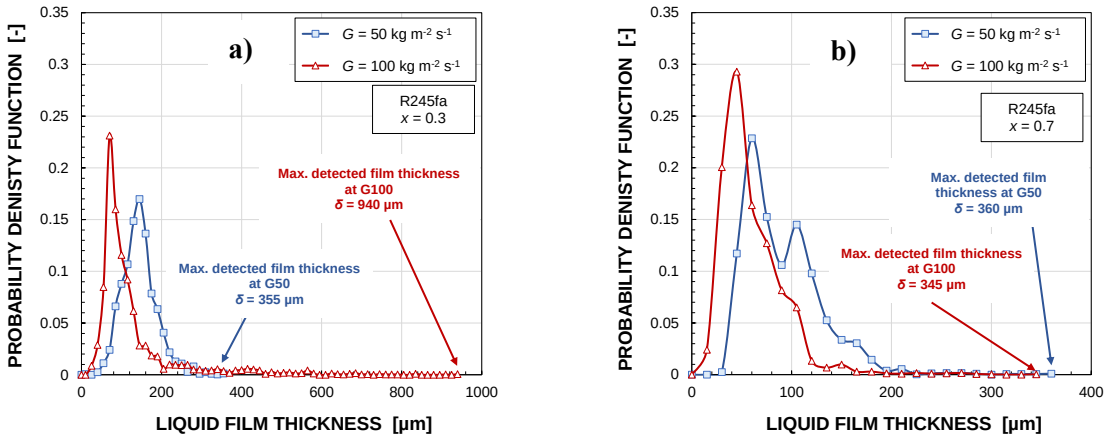

Figure 2. Probability density functions of liquid film thickness at mass velocity G equal to 50 and 100 kg m^{-2} s^{-1}. a) Vapor quality x = 0.3, b) vapor quality x = 0.7.

The instantaneous values of the liquid film thickness can be analysed by calculating the mean and the base liquid film thickness. The first one (δ_{mean}) is intended as the average of the instantaneous thickness values measured during the acquisition time (3.1 s), while the second one (δ_{base}) represents the mean height of the liquid substrate between subsequent high-amplitude waves. In fact, high-amplitude waves, referred in the literature as "disturbance waves", are found to appear in some conditions (G = 100 kg m^{-2} s^{-1} and $x < 0.5$). Disturbance waves carry a significant portion of the condensate promoting the thinning of the residual liquid film and thus affecting the condensation heat transfer. In Figure 3, the experimental heat transfer coefficient HTC$_{exp}$ measured in the 3.4 mm diameter tube is compared to the heat transfer coefficient HTC$_{calc}$ calculated as:

$$\mathrm{HTC}_{calc} = \frac{\lambda_L}{\delta} \tag{2}$$

where λ_L is the liquid thermal conductivity and δ is the mean/base film thickness. At $x \approx 0.3$, the heat transfer coefficient calculated considering δ_{base} is about 24-30% lower than the experimental one for the tested mass fluxes, while a much higher difference is obtained if considering δ_{mean}. This means that heat transfer must be enhanced by the turbulence in the base liquid film and by the recirculation zones inside the disturbance waves (Jayanti and Hewitt [9]). At $x \approx 0.7$, the heat transfer coefficient calculated with

δ_{base} deviates by less than 12% from the measured one for the tested mass fluxes. Therefore, when increasing the vapour quality, conduction through the liquid film is the main contribution and thus the increase of the heat transfer coefficient is mainly due to the thinning of the liquid film.

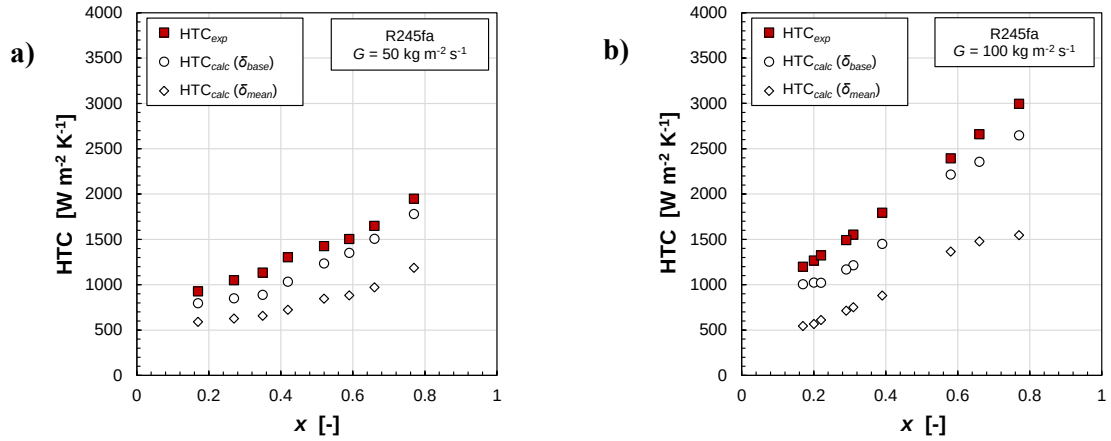

Figure 3. Experimental heat transfer coefficient (HTC_{exp}) and calculated heat transfer coefficient (HTC_{calc}) considering purely conductive heat transfer in the laminar liquid film (measured base and mean liquid thickness values are used). a) Mass velocity G = 50 kg m^{-2} s^{-1}, b) mass velocity G = 100 kg m^{-2} s^{-1}.

4. Conclusions

Condensation heat transfer coefficients and liquid film thickness have been measured during R245fa vertical downward flow inside a 3.4 mm inner diameter tube. The condensation process has been studied at 40 °C saturation temperature and mass velocities equal to 50 and 100 kg m^{-2} s^{-1}. The flow pattern visualizations show that the flow is always annular with waves of different amplitude depending on the operative conditions. In particular, high-amplitude disturbance waves are observed at low vapour quality and high mass flux. The measured heat transfer coefficient is higher compared to the heat transfer coefficient calculated assuming only thermal conduction in liquid (laminar) film. This can be explained considering presence of turbulence in the base liquid film and in correspondence of disturbance waves. The experimental heat transfer coefficient is found to increase with vapour quality and this is related to the thinning of the liquid film induced by vapour shear stress.

Acknowledgments

The European Space Agency is acknowledged for its financial support through the MAP Condensation program ENCOM-4 (AO-2004-096). The authors also acknowledge the financial support of the Department of Industrial Engineering of the University of Padova through the project BIRD187743.

References

[1] Toninelli P, Bortolin S, Azzolin M and Del Col D 2019 *Heat Transf. Eng.* **40**(9-10) 802–817
[2] Azzolin M, Bortolin S and Del Col D 2019 *Int. J. Heat Mass Transf.* **144** 118646
[3] Cioncolini A, Del Col D and Thome J R 2015 *Int. J. Multiph. Flow* **75** 26–38
[4] Tibiriçá C B, do Nascimento F J and Ribatski G 2010 *Exp Therm. Fluid Sci.* **34** 463–473
[5] Mederic B, Lavieille P and Miscevic M 2005 *Exp. Therm. Fluid Sci.* **30** 785–793
[6] Han Y, Kanno H, Ahn Y J and Shikazono N 2015 *Int. J. Multiph. Flow* **73** 264–274
[7] Lemmon E W, Huber M L and McLinden M O 2013 *NIST Standard Reference Database 23: Reference Fluid Thermodynamic and Transport Properties-REFPROP, Version 9.1*
[8] Berto A, Lavieille P, Azzolin M, Bortolin S, Miscevic M and Del Col D 2021 *Int. J. Multiph. Flow* **140** 103649
[9] Jayanti S and Hewitt G F 1997 *Int. J. Heat Mass Transf.* **40** 2445–2460